

BRIDGING SCALE GAPS IN MULTISCALE MATERIALS MODELING IN THE AGE OF AI

Machine Learning-Driven Identification of Favorable Dopants for Activating Non-basal < c + a > Slip in Mg Alloys

YIDI SHEN, 1 YUFENG HUANG, 2,3 and QI AN1,4

1.—Department of Materials Science and Engineering, Iowa State University, Ames IA 50011, USA. 2.—School of Professional Studies, Columbia University, New York, NY 10027, USA. 3.—e-mail: yh3584@columbia.edu. 4.—e-mail: qan@iastate.edu

Activating non-basal $\langle c + a \rangle$ slip is essential to enhance the ductility and formability of Mg alloys at room temperature. To determine favorable dopant species for lowering the energy barrier of $(10\overline{1}1)$ slip system in Mg alloys, we trained various machine learning models using a dataset from 106 distinct elemental species and 29 unique calculations obtained from density functional theory (DFT). The models, including regression decision trees, random forest, and linear and polynomial regression, prioritized features affecting the unstable stacking fault energy (USFE) of the slip system, crucial for activating non-basal $\langle c + a \rangle$ slip. A third-degree polynomial regression model was selected for its acceptable accuracy without significant overfitting, enhanced by Shapley values to determine the most significant features affecting the USFE. The forces on Mg atoms adjacent to the dopant, the angle formed by adjacent Mg in relation to the dopant atom, and localized charges on the adjacent atoms to the dopant emerged as significant for determining the USFE. The predictive capability of the model was validated using lasso regression, showing accurate prediction of the USFE values for ternary Mg alloys. Our model provides a strong baseline system for determining successful alloying combinations to potentially enhance Mg ductility at room temperature.

INTRODUCTION

The search for lightweight, high-strength structural materials is one of the major research areas of materials science today. Magnesium (Mg) and Mg-based alloys have a very high strength-to-weight ratio but suffer from a significant lack of room temperature ductility due to the limited activated non-basal < c + a > slip systems. Most Mg alloys, particularly Mg-Al alloys, must be worked at higher temperatures than similar materials, leading to increased energy expenditures in their manufacturing process that are undesirable for widespread applications. Most efforts to improve the room-temperature ductility of Mg-based materials focus on alloying or treatments that stabilize the formation of pyramidal dislocations, which tend to form sessile locks after dispersing into the basal (0001)

plane.^{5–11} These include alloying with rare earth elements such as ytterbium, ¹² gadolinium, ¹³ and lanthanum ¹⁴ as well as the introduction of nanoparticles through powder metallurgy approaches to mitigate the limiting mechanical characteristics inherent to Mg and Mg-based alloys, such as improving yield stress and increasing tensile strength through intermetallic formation as well as changing corrosivity due to the increased porosity of the nanoparticles. ^{15–17} Despite extensive research, to date, no cost-effective and practical enhancement technique has been found to allow widespread adoption of Mg-based materials for areas such as structural materials, aerospace applications, and industrial uses.

Experimental research for improving Mg-based materials is limited because it is relatively expensive and time-consuming compared to computational techniques. As such, extensive computational research has been conducted on searching alloying candidates for improving the mechanical properties of Mg, particularly with

Published online: 10 July 2024

density functional theory (DFT) simulations to identify changes in the stacking fault energies (SFEs) for the most-active non-basal slip systems in the $(10\overline{1}1)$ and $(11\overline{2}2)$ slip planes. ^{19–21} Many studies have been performed for the screening of dopant elements suitable for improving the ductility of Mg by lowering the energy barriers for activating pyramidal slip using DFT simulations, 22-24 but comprehensive analysis of effective dopants has been more limited by constrained selection of candidate elements, particularly for models with more than one dopant, primarily because of expensive computational cost and small supercell in DFT. 25,26 The application of effective high-throughput screening methods (HTS) to select ideal dopant candidates in this manner may require significant computational resources⁶ and can also be time-consuming. Consideration of systems containing multiple dopant elements further complicates these problems; an effective solution to these concerns is the application of machine-learning (ML) methods to quickly predict suitable dopant elements in lieu of direct calculation methods.

Machine learning (ML) methods are particularly valuable in this type of research because of their ability to provide fast, accurate, and interpretable predictions of related chemical structures based on existing DFT calculations. Various ML techniques have been applied to design materials with desired properties ^{27,28} and to develop new catalysts. ^{29,30} Notably, methods such as polynomial regression, ridge regression, and support vector regression have been extensively used to study multi-element and disorder-containing alloys.³ For instance, ridge regression using the L2 norm has been employed to predict the energetics and kinetics of Cr atoms in Fe-Ni-Cr alloys, considering local electronegativity and atomic packing environments.³¹ Additionally, XGBoost has been effectively utilized to predict promising intermetallic compounds that can suppress the corrosion cathodic reaction in Mg alloys by reducing hydrogen adsorption energy, achieving a mean absolute error (MAE) of 0.196 eV. 32 Moreover, the stacking fault energies (SFEs) of alloys have been explored using ML methods combined with DFT simulations. 33,34 For example, Gaussian process regression (GPR) with an MAE $< 8\ mJ/m^2$ was used to predict the SFEs of dilute FCC-based alloys, including Al-, Ni-, and Pt-based alloys.³³ Among 49 elemental features, the covalent radius, followed by the electronic structure, plays a significant role in regulating SFEs.

Here, we target the prediction of the unstable stacking fault energies (USFE) in the general stacking fault energies surface (GSFES) for correlating dopants with potential increases in the probability of activating non-basal $\langle c + a \rangle$ slip in Mg alloys. Terating effective ML models requires a significant number of initial calculations for the

construction of an effective dataset for training the model along with appropriate model selection. ^{36–41} Due to the limited pool of useful dopant elements for industrial (low cost, relatively non-toxic, capable of alloying, etc.), this means that careful feature selection and comprehensive DFT analysis of single-element dopants for the most relevant slip systems is required to train a model for the prediction of systems with multiple dopant elements. Additionally, the complexity of ternary doping systems in Mg must be carefully considered (most effective doping sites, feature determination with multiple dopants, etc.).

In this work, we trained a variety of ML models using a DFT-calculated dataset of properties from 106 distinct dopant elements in the Mg ($10\overline{1}1$) slip plane to determine the most effective ML model for this particular problem. A trained polynomial regression model was determined to be most effective from which important features from a pool of 29 total features to aid in interpreting the physical meaning behind the predicted most suitable species for improving the activation of non-basal $\langle c + a \rangle$ slip systems. A further adaptation of the model using polynomial regression with lasso regularization techniques was used to predict the USFE for various ternary alloys containing two dopants selected from the previously determined most suitable candidates²⁶ to a high degree of accuracy compared to the DFT-determined values (within 10%). This model can be improved for use with a wide variety of alloy systems in future studies for determining suitable dopant combinations to improve the activation of non-basal $\langle c + a \rangle$ slip systems using a similarly determined initial feature set from DFT calculations.

COMPUTATIONAL METHODS

ML Models

Several machine learning models were trained using the data set derived from DFT and literature, 26,42,43 including decision tree, random forest, and both linear and polynomial regression. The decision tree and random forest models were prepared using the regression decision tree implementation and random forest classifier implementation of sklearn, 44 respectively. These models were created using random splitter criteria and a train-test splitting of the data set of 90-10. Initial feature importance evaluation was prepared using sklearn and XGBoost⁴⁵ and required a larger train-test split of 80-20 for satisfactory results in conjunction with the gradient boosting feature importance calculation technique. This feature involves two primary calculation methods: gain, which uses the averaged relative contribution of each feature to the decision tree model from the native xgboost implementation and permutation feature importance using sklearn integration in which features are weighted in

importance after randomization based on their impact on the model across many iterations. Next, linear and polynomial regression models were trained for the purpose of predicting the USFE in ternary systems using the sklearn implementation using the features directly as input. We then used principal component analysis (PCA)^{46,47} to generate a suitable set of principle components to simplify the model by reducing dimensionality as well as determine collinearity trends among the feature types (charge, element-specific, angles and distances, etc.) used in the model. Hyperparameters were optimized using the grid-search approach with five-fold cross validation⁴⁶ and were conducted for all relevant combinations of hyperparameters in the regression models to determine the optimal configuration for the lowest root mean squared error (RMSE) results and optimized R2 value. Additional consideration was given to the issue of overfitting in the higher-order polynomial regression models using our complex data set by limiting the degree of the polynomial to fifth or lower; higher degrees were found to result in significant overfitting to outliers in the data set even with the inclusion of regularization terms and thus rendered the model less useful for predicting the USFE. Significant improvements in model accuracy were obtained with a combination of lower-order polynomial regression in conjunction with regularization methods compared to higher-order polynomials. The error calculation method can be found in the online Supplementary Materials.

Polynomial Regression

Features were pre-processed to standardize the variance of each feature to a mean of near-zero and a standard deviation of one, to homogenize the disparate feature values for use in both linear and polynomial regression model, and to ensure a more regular distribution of the data set while preventing significantly larger values corresponding to certain features from affecting the accuracy of the regression model. Models were prepared using PCA to reduce the number of input features while still using the full 29 feature data set. A hyperparameter search found that PCA-enabled polynomial regression using a third-degree polynomial with 14 principal components (PCs) provided the lowest RMSE and thus most accurate predictions. Finally, Shapley values were calculated using the SHAP implementation⁴⁶ assigned to the PCs to determine the most significant combinations of features for affecting the USFE, which correlates with a change in ductility for the Mg alloys.

Ridge and Lasso Regression

After initial predictions of the USFE values for ternary systems were made using the trained polynomial regression model, it was further refined usinh lasso⁴⁷/ridge⁴⁷ regularization modifiers using their native implementation in sklearn. Lasso regression alters the regression model by introducing a term representing the absolute weight of each feature (commonly known as the L1-penalty or L1norm), while ridge regression introduces a similar term representing the squared weight of the features (known as the L2-penalty or L2-norm). In both methods, a hyperparameter denoted by alpha was used to determine the strength of the regularization, such that alpha equals 0 is equivalent to no regularization. Thus, a final grid search was performed to find the optimized alpha terms for each model. Lasso regression was found to be unsuitable for use because of its well-known issues with datasets that are highly collinear, such as ours, and provided minimal improvement in the accuracy of the predicted USFE for ternary systems compared to the calculated DFT values. However, ridge regression using an alpha parameter of 5.2 produced an average increase in accuracy of 2.4% for predicted USFE values compared to those from ordinary polynomial regression.

DFT Methods

The VASP periodic code 48,49 was utilized to conduct all DFT simulations. The electronic exchange-correlation interaction was described using the Perdew-Burke-Ernzerhof (PBE) 50 functional's generalized gradient approximation (GGA). The corevalence interaction was represented using the projector augmented-wave (PAW) method. 51 The self-consistent field and geometry optimization convergence criteria were set to $10^{-5}\,\mathrm{eV}$ and $10^{-2}\,\mathrm{eV/Å}$, respectively. The plane-wave expansion's energy cutoff was set at 500 eV. The Kohn-Sham energies were sampled across the Brillouin zone using a $3\times7\times1$ Monkhorst-Pack grid scheme for $(10\overline{1}1)$, respectively.

Based on our previous DFT simulations, ²⁶ doping different elements at these two sites leads to different effects on USFE values. Particularly, for the most promising candidates (Te, Bi, Sb, Pb, and Tl), which exhibit the lowest USFE values among all possible dopants, we found that their USFE values at both sites are lower than those of pure Mg. Additionally, the USFE is lower at site 1 compared to site 2 (Fig. 1), suggesting that site 1 might be the more plausible site for unstable stacking faults structures. In addition to the data from our previous work, 26 we further incorporated the ternary systems (with two doping elements) also into our calculations to validate the effectiveness of our ML model. We first constructed slab models for the $(10\overline{1}1)$ plane. Particularly, the model of $(10\overline{1}1)$ plane was obtained by orientating the unit cell along $[\overline{1}2\overline{1}0]$ (a axis) and $[11\overline{2}3]$ (b axis) directions. A vacuum of 20 Å in the z direction was incorporated to minimize potential interactions among the replicated images. A $2 \times 2 \times 1$ supercell slab model was

Slip System: (1011) plane

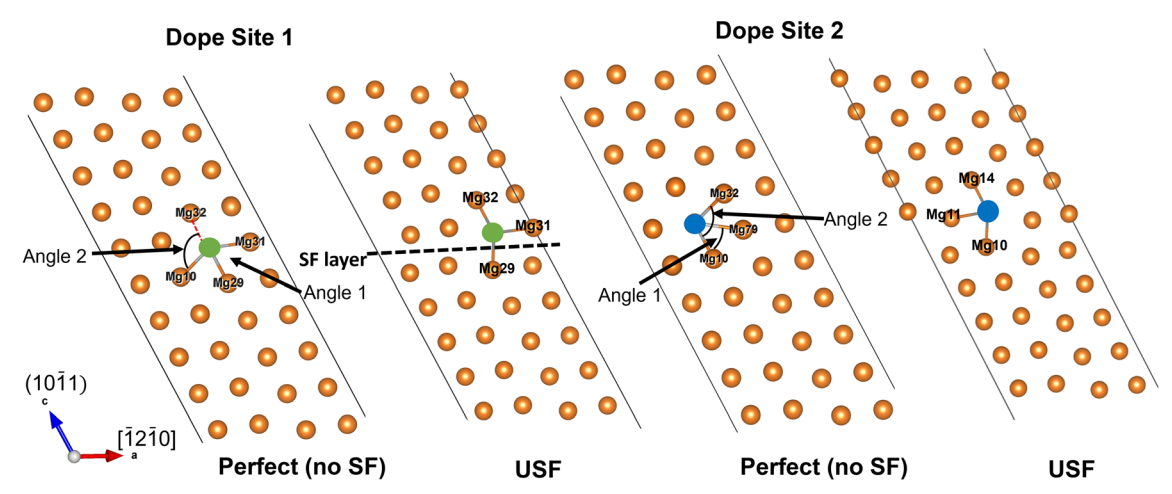


Fig. 1. The $(10\overline{1}1)$ slip system in Mg metal. Two optimal dopant sites were studied using DFT methods in the original work, from which the data set of 106 tested dopant elements with 29 features of interest is derived relating to the forces, charges, bond angles, bond distances, and attributes of the dopant elements relative to the adjacent Mg atoms.

created, leading to the models comprising 80 atoms for the $(10\overline{1}1)$ plane. This is a configuration analogous to our binary-doped structures depicted in Fig. 1. Subsequently, two Mg atoms in close proximity to the stacking fault plane were replaced by doped elements to form the ternary structures. For the $(10\overline{1}1)$ plane, two distinct atomic sites exist within stacking fault plane (as illustrated in Fig. 1), indicating two potential doping sites. Hence, we scrutinized all attributes and GSFE values of structures integrating two dopant elements at both sites.

The data set used in this study consists of DFTderived values for structures representing the $(10\overline{1}1)$ slip system in Mg allov containing a single dopant of another element. Two optimal potential doping sites were determined in previous work,² and features were determined from both the "perfect" system with no stacking fault (SF) and the unstable stacking fault (USF) configuration for both dopant locations (shown in Fig. 1, above). For the 106 distinct dopant species analyzed with DFT techniques, data for 29 distinct features relating to the position, bond angles, elemental attributes of the dopant (atomic mass, electronegativity, atomic radius, etc.), forces (in x, y and z directions), and charges on the dopants and adjacent Mg atoms were determined as well as the unstable stacking fault energy (USFE) for each dopant species in each system. To determine the Mulliken charge for all Mg alloys, the crystal orbital Hamilton population (COHP)⁵² implemented in the LOBSTER package⁵³ was employed. The DFT-derived dataset for both binary and ternary-systems used in developing the ML model can be found in Supplementary Materials.

RESULTS AND DISCUSSION

Our initial efforts in creating a ML prediction of useful features for determining the effect of elements on improving activation of non-basal $\langle c + a \rangle$ slip of Mg alloy using DFT-derived data focused on simple classification methods that are capable of directly determining feature importance. This was decided because of the limited size of our data set; a small data set is highly prone to overfitting with most common ML techniques. These included decision tree regression and random forest classification using the sklearn implementation, both of which are straightforward techniques well suited for complex data sets of intermediate size. A standardized 90/10 randomized train-test split for the data set was used in both models with the USFE as the predicted (y) value and the other features as the predictor (x) values across many iterations using different randomization states employed to ensure effects relating to the small size of the data set were minimized.

Interestingly, several key features were identified by both models, including the bond angle between Mg-32, the dopant and Mg-10, the charges on Mg-31 and Mg-10, and the distance between Mg-31 and the dopant in both studied dopant positions for the (1011) slip system. The positions of these Mg atoms and dopants can be found in Fig. 1. A simplified representation of the decision tree model is shown in Fig. 2. The relative simplicity of the models coupled with high RMSE values (averaging 29% in the random forest model and 34% in the decision tree model), however, indicated the unsuitability of these methods for analyzing this data set. Additionally, high variance between randomization states indicated that significant overfitting was occurring.

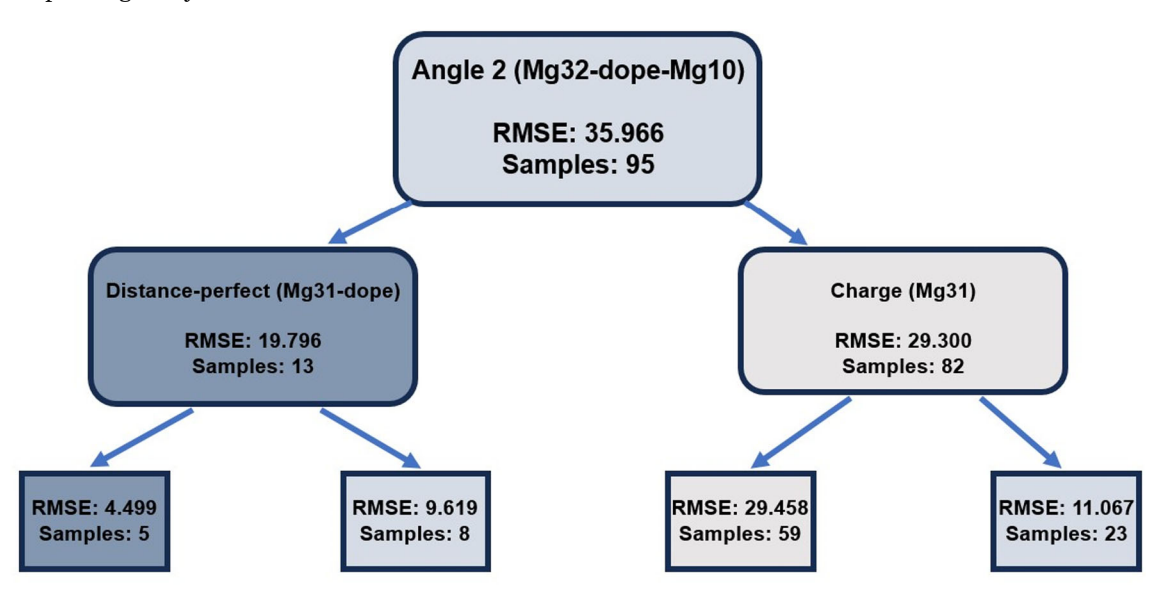


Fig. 2. Root mean squared error (RMSE) regression decision tree results. The root node is determined using the highest RMSE feature as the 'most important feature' for classifying the data set. Subsequent 'important' branching nodes are implemented according to the algorithm, resulting in the decision tree. The feature name, criterion for the node, mean squared error, number of samples passing the node, and importance value are shown on each node. The tree pictured is simplified for the sake of clarity. Darker shading for nodes indicates lower RMSE for features classified under that node.

Further development of a suitable ML model for evaluating the doped Mg system was directed towards the use of regression methods.

The next step in our model development was fitting the dataset to regression-based models to combat the limiting characteristics encountered in the previous models. Considering a combination of simple linear regression models and more complex polynomial regression models, polynomial regression was found to be more suitable at interpreting the relatively complex data set. This was expected, as the 29 initial features ranging from atomic characteristics inherent to the element to DFT-derived features are understood to encompass many non-linear relationships which are more easily expressed through a polynomial regression model.

SHAP values are a method of assigning local feature importance that is unscaled by weights inherent to the model type they are applied to, allowing the importance of specific features to be calculated independently for each element in relation to the whole model. To this end, SHAP values were calculated using an initial polynomial regression model of a low degree (≤ 4) to help mitigate overfitting issues and all 29 initial features in the dataset to determine the most-relevant features so that we may better understand the relation these features have with USFE in the doped Mg system. Figure 3 shows the calculated SHAP values, indicating contrasting results to those of the decision tree model. The ten most important features are displayed in Fig. 3. A larger variance in SHAP values indicates a more significant feature in the model. Specifically, the atomic forces on Mg 31, Mg 29, and Mg10, which are near the dopant, play a

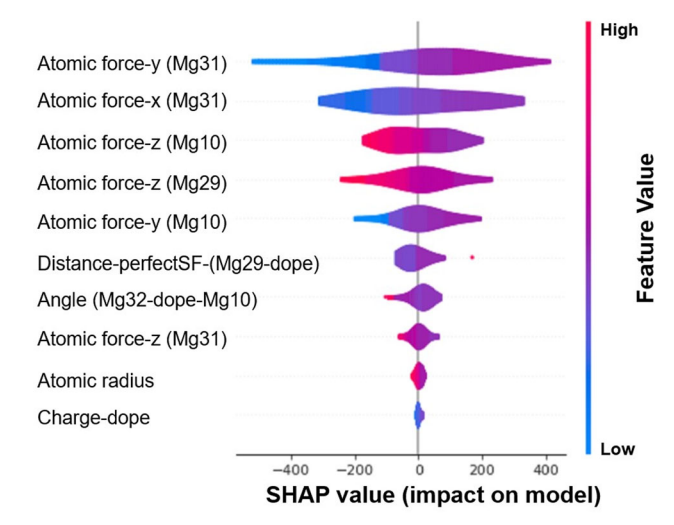


Fig. 3. Calculated SHAP values for the most-relevant (largest variance in SHAP value) features using a polynomial regression model.

dominant role in the polynomial regression model. In contrast, the charge of the dopant, atomic radius, atomic distance between the dopant and Mg 29, and angles are much less important compared to the top five force features. Overall, bond angle 1 (shown in Fig. 1) and the atomic forces acting on adjacent Mg atoms to the dopant were found to be significant along with the related distances relative to the dopant. Interestingly, in the polynomial regression model the removal of the charge-related features and retraining of the model were both found to significantly affect the accuracy of the model as well as the ordering of the feature importance. In the absence of the charge terms, the atomic distance of

the adjacent Mg atoms was found to significantly increase in importance while the two significant angles relevant to the doping position decreased in importance. This indicates a strong non-linear relationship between the charge terms and the other relevant features for selecting a suitable ductility-enhancing candidate. However, incorporating nonlinear and interaction terms using all of the 29 original features in polynomial forms will create too many features; it is thus important to reduce the dimensionality of the problem. One way to reduce the dimensionality is to remove features based on the SHAP values of the features. However, this approach creates an arbitrary cutoff to choose from the original features that could lead to artificial errors. Rather than reducing dimensionality arbitrarily using the SHAP values, we leveraged PCA to choose different linear combinations of features so that even features with small SHAP values could be incorporated into the ML model.

The use of feature scaling (with mean of near-zero and standard deviation of one) to employ PCA for generating PCs to simplify the initial feature assortment into a reduced number of 'effective features' was thus determined to be a suitable next course of action. After limited initial testing, the use of 10 PCs was found to capture $\sim 93\%$ of the total variance of the data set, while increasing to 20 PCs was found to capture 99.8% of the variance. A grid search to find the optimized hyperparameters for sklearn's linear regression, polynomial regression, lasso regression, and ridge regression using both linear/polynomial regression models was then employed; the hyperparameters considered were the models themselves in addition to the total number of PCs produced by PCA on the data set as well as the polynomial degree in polynomial models, normalization status in linear regression, and alpha modifier for lasso regression. PCs from 1 to 24 were considered (~37% to 99.96% of total data set variance captured) for the grid search across many initial randomized states to ensure unbiased results, while polynomial degrees for relevant model options were limited to 4 or below as higher degrees were found to significantly overfit the model in preliminary testing. Additionally, alpha selection ranging from 0.001 to 100.0 was used for lasso regression optimization, and alpha selection ranging from 0.1 to 10 was used for ridge regression optimization. Five-fold cross validation employed for the grid search. Overall, the removal of charge-related features and retraining significantly affected the accuracy and feature importance order in the polynomial regression model. Without charge terms, the importance of the atomic distance of adjacent Mg atoms increased, while significant angles decreased, indicating a non-linear relationship between charge and other features. PCA was deemed suitable for simplifying the model, reducing the feature set to 29 without compromising integrity. Using PCA, 10 PCs captured ~ 93\% variance,

and 20 PCs captured 99.8%. In various regression models, considering PCs and a small polynomial degree (≤ 4) improves accuracy and helps in addressing overfitting in our ML models.

The results of the grid search indicated that lasso regression was unfavorable, as the smallest alpha score possible was always selected during the grid search as the favorable hyperparameter. This indicates some co-reliance between PCs/features in the data set that is poorly interpreted by regularization terms in lasso regression models. Likewise, poor R^2 correlation values for standard linear regression were obtained using the optimized hyperparameter combination suggested; relatively good results were found instead for the polynomial regression and ridge regression methods. A comparison of the predicted USFE values in polynomial regression, polynomial regression with ridge regression, and polynomial regression with lasso regression is shown in Fig. 4. The abbreviated results of the grid search for the polynomial regression implementation in sklearn are shown in Table I below; using the optimized combination of hyperparameters in a modified polynomial regression model resulted in an average test RMSE of 4.49 score with a R^2 value of 0.93. We thus concluded that polynomial regression performed with 10-18 PCs using a third-degree polynomial with normalization produces optimal results for this model. The entirety of the principal components data found in Table I is shown in Supplementary Table SI. Notably, some smaller errors for polynomial regression may come with a limited testing data pool.

To test the applicability of the now-trained model, DFT data from select ternary systems including dopants chosen from the most suitable for

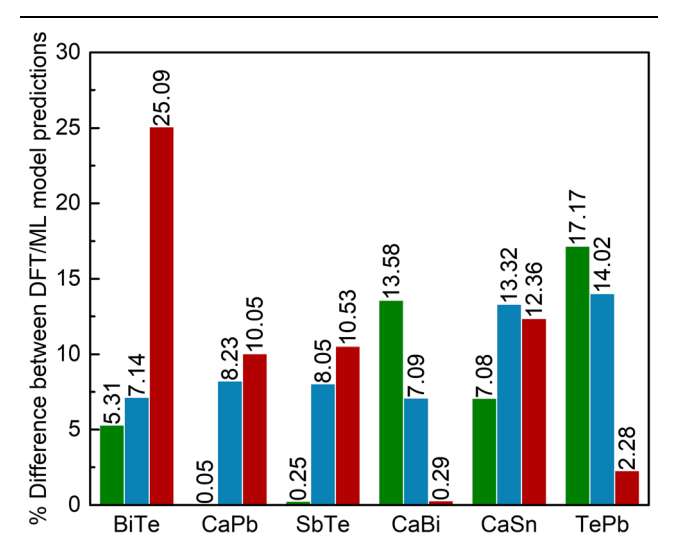


Fig. 4. Comparison of model accuracy for six selected doped system predictions. The blue bar represents the unaltered polynomial regression model with n=3 and #pc=14, while the green bar represents the same model with ridge regression (alpha = 5.2) and the red bar represents the same model with lasso regression (alpha = 0.001); the optimal parameters were determined from hyperparameter optimization (Color figure online).

Table I. Grid search results for polynomial	regression	using the	Mg	ductility	data	set.	Full	results	are
available in Supplementary Table SI									

# PCs	Training RMSE	Polynomial degree/ normalization	Dataset variance captured (%)	Test RMSE	R^2 value
1	24.35	2, False	37.0	19.14	$-\ 0.1$
2	18.49	3, True	51.1	26.72	0.13
3	14.14	2, False	64.7	15.71	0.23
13	0	3, True	97.2	9.99	0.69
14	0	3, True	97.9	5.64	0.90
15	0	3, True	98.6	5.82	0.89
16	0	3, True	99.0	6.23	0.88
21	0	2, False	99.9	14.59	0.34
22	0	2, False	99.9	13.79	0.41
24	0	2, False	99.9	13.76	0.42

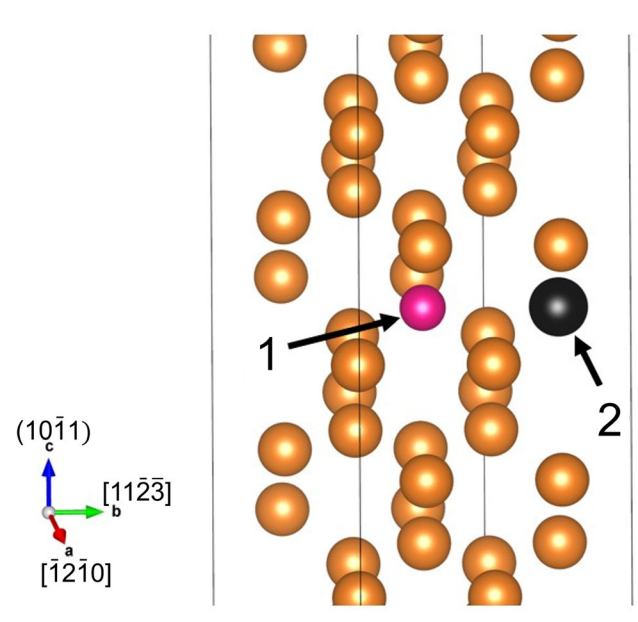


Fig. 5. Representation of primary dopant position (1, pink) and secondary dopant (2, black) in the (1011) computational model. Feature selection for relevant features (element-specific, adjacent Mg distances and charges, primary and secondary angle, atomic forces) is determined relative to the dopant position 1 for ML model (Color figure online).

increasing ductility in previous works^{23,44} were tested in the model to predict the USFE. The ternary system provided several unique challenges for feature selection; with two distinct dopants the selection of doping position for the features that rely on the doping position (distances, element-specific features such as atomic mass, charges on the dopant and adjacent Mg atoms, etc.) was found to create a significant difference in the accuracy of the predicted USFE. Selection of all relevant features based on the central doping position (site 1 in Fig. 5) for the Mg system resulted in increased accuracy compared to selecting features based on the secondary doping position (shown in Fig. 5 as site 2). Therefore, we consider doping site 1 (Fig. 5)

as the primary site in our model, and all features are based on the dopant in site 1. Notably, site 2 is one of the nearest neighbors of site 1, and the features of the second dopants (e.g., mass, charge, etc.) can be included in our model. Decent accuracy was obtained using the previously described polynomial regression model (n=3 and #pc = 14); to increase the accuracy of the predictions, ridge regularization was used with an alpha parameter of 5.2 to significantly increase the accuracy of predictions for the selected ternary-doping systems. The predicted USFE values are shown in Table II below with comparison to their DFT-calculated USFE.

As shown in Table II, accurate prediction of the DFT-calculated USFE values using the ML model is limited; certain combinations of dopants are accurately predicted to be within a fraction of a percentage difference from the DFT value while others vary by up to 13.58%. The single high-error ternarydoping combination tested was Ca-Bi-Mg, for which the immediate reasons behind its deviance from the other ternary combinations are unclear. Other combinations including large-sized dopants in the interior doping position (such as Bi, Ca and Pb) are uncorrelated with the prediction error, as well as systems having an elevated charge disparity between adjacent Mg atoms. Similarly, the differences in the primary and secondary angles (shown in Fig. 1 as Angle 1 and Angle 2) seem not to correlate to the prediction accuracy. However, a discrepancy in the forces acting on the primary dopant (the dopant located in the central position in the model), as illustrated in Fig. 5, in the x direction (or the slip direction) seems to indicate that species with the lowest atomic force results in the highest calculated error relative to the DFT prediction for that dopant combination. This indicates that the polynomial regression model with ridge regression parameters is influenced by the force terms in the features, with a more-complicated relationship to the other features that may be difficult to directly explain. Further testing using DFT data from other

Table II. Predicted USFE of ternary system predictions using polynomial regression with and without ridge regularization compared to calculated USFE values from DFT

System	USFE (DFT)	USFE (PR)	% Diff. (PR)	USFE (PR w/ridge)	%Diff (PR w/ridge)
Bi-Te-Mg	131.66	141.39	7.13	138.84	5.31
Ca-Pb-Mg	179.52	165.33	8.23	179.44	0.05
Sb-Te-Mg	139.96	129.12	8.05	140.32	0.25
Ca-Bi-Mg	164.19	176.27	7.09	188.12	13.58
Ca-Sn-Mg	184.16	161.17	13.32	171.57	7.08

Percent difference for both models is shown; use of ridge regularization is found to reduce overall difference in predicted value from calculated value.

dopant combinations in Mg may help illuminate the cause of the error discrepancy for the model in the future.

CONCLUSION

Improving the ductility of Mg using elemental dopants is a key area of computational research to eliminate the high-cost and time-consuming experimental methods necessary for direct testing of these systems. The implementation of machine learning methods, such as those described in this work, can help simplify the tremendous computational resource consumption required for calculating the necessary parameters using methods such as DFT by reducing the number of calculations required to those needed for constructing a suitable training dataset. Through predictions with the prepared machine learning model, suitable ternarydoped systems for full DFT analysis can be pinpointed out of the multitude of combinations from previously identified binary-doped candidates, thus saving considerable time and resources from doing blanket direct calculations. We find that polynomial regression models using regularization techniques produce reasonably accurate USFE predictions in most cases in the $(10\overline{1}1)$ slip system most likely to produce pyramidal slip in the Mg system beneficial to improving ductility. Additionally, we find the charge on adjacent Mg atoms to the dopant species and their relative distances from the dopant play important roles in the ML model's predictions, indicating a necessary base level of features required for the training data set. This type of ML model can be further refined and used for similar ductility-enhancing research to determine suitable alloy combinations for other metals in the future.

SUPPLEMENTARY INFORMATION

The online version contains supplementary material available at https://doi.org/10.1007/s11837-024-06728-7.

ACKNOWLEDGEMENTS

This work was supported by NSF 2032483.

CONFLICT OF INTEREST

The authors declare that they have no known conflicts of interest, financial or personal, that influenced the results reported in this work.

REFERENCES

- H. Pan, Development and Application of Lightweight Highstrength Metal Materials. Paper Presented at the International Conference on Metal Material Processes and Manufacturing (ICMMPM 2018), Jeju Island, South Korea, vol. 207 (2018), p. 3010.
- B.L. Mordike and T. Ebert, Mater. Sci. Eng. A 302, 37 (2001).
- U.M. Chaudry, K. Hamad, and J.-G. Kim, J. Alloys Compd. 792, 652 (2019).
- 4. T.M. Pollock, Science 328, 986 (2010).
- H. Yoshinaga and R. Horiuchi, Trans. Jpn. Inst. Met. 5, 14 (1964).
- R. Ahmad, B. Yin, Z. Wu, and W.A. Curtin, *Acta Mater.* 172, 161 (2019).
- 7. Z. Wu and W.A. Curtin, Nature 526, 62 (2015).
- F. Kang, Z. Li, J.T. Wang, P. Cheng, and H.Y. Wu, J. Mater. Sci. 47, 7854 (2012).
- 9. J. Koike, T. Kobayashi, T. Mukai, H. Watanabe, M. Suzuki, K. Maruyama, and K. Higashi, *Acta Mater.* 51, 2055 (2003).
- 10. R.E. Reed-Hill and W.D. Robertson, JOM 9, 496 (1957).
- 11. E.C. Burke and W.R. Hibbard, JOM 4, 295 (1952).
- P. Gunde, A.C. Hänzi, A.S. Sologubenko, and P.J. Uggowitzer, *Mater. Sci. Eng. A* 528, 1047 (2011).
- H. Ovri, J. Markmann, J. Barthel, M. Kruth, H. Dieringa, and E.T. Lilleodden, Acta Mater. 244, 118550 (2023).
- N. Stanford and M.R. Barnett, Mater. Sci. Eng. A 496, 399 (2008).
- J. Alias, W.S.W. Harun, and H.M. Ayu, KEM 796, 3–10 (2019).
- H. Watanabe, T. Mukai, M. Mabuchi, and K. Higashi, *Acta Mater.* 49, 2027 (2001).
- S. Ignat, P. Sallamand, D. Grevey, and M. Lambertin, *Appl. Surf. Sci.* 225, 124 (2004).
- W. Gao, H. Liu, and I.O.P. Conf, Ser. Mater. Sci. Eng. 4, 012003 (2009).
- J.R. Morris, J. Scharff, K.M. Ho, D.E. Turner, Y.Y. Ye, and M.H. Yoo, *Philos. Mag. A* 76, 1065 (1997).
- A. Datta, U.V. Waghmare, and U. Ramamurty, *Acta Mater*. 56, 2531 (2008).
- M. Muzyk, Z. Pakiela, and K.J. Kurzydlowski, Scr. Mater. 66, 219 (2012).

Machine Learning-Driven Identification of Favorable Dopants for Activating Non-basal $\langle c + a \rangle$ Slip in Mg Alloys

- X. Wu, R. Wang, and S. Wang, Appl. Surf. Sci. 256, 3409
- Z. Wu and W.A. Curtin, Scr. Mater. 116, 104 (2016).
- 24.R. Namakian, G.Z. Voyiadjis, and P. Kwaśniak, Mater. Des. 191, 108648 (2020).
- S. Sandlöbes, M. Friák, S. Korte-Kerzel, Z. Pei, J. Neugebauer, and D. Raabe, Sci. Rep. 7, 10458 (2017).
- Y. Shen, H. Wang, B. Li, and Q. An, Phys. Rev. Mater. 3, 53603 (2019).
- J. Wei, X. Chu, X. Sun, K. Xu, H. Deng, J. Chen, Z. Wei, and M. Lei, InfoMat 1, 338 (2019).
- 28. S.M. Moosavi, K.M. Jablonka, and B. Smit, J. Am. Chem. Soc. 142, 20273 (2020).
- A.F. Zahrt, J.J. Henle, B.T. Rose, Y. Wang, W.T. Darrow, 29. and S.E. Denmark, Science 363, 247 (2019).
- W. Yang, T.T. Fidelis, and W. Sun, ACS Omega 5, 83 (2020).
- Y. Wang, B. Ghaffari, C. Taylor, S. Lekakh, M. Li, and Y.
- Fan, Scr. Mater. 205, 114177 (2021). Y. Wang, Q. Tang, X. Xu, P. Weng, T. Ying, Y. Yang, X. Zeng, and H. Zhu, Acta Mater. 255, 119063 (2023).
- X. Chong, S. Shang, A. Krajewski, J.D. Shimanek, W. Du, Y. Wang, J. Feng, D. Shin, A.M. Beese, and Z. Liu, J. Phys. Condens. Matter 33, 295702 (2021).
- T.Z. Khan, T. Kirk, G. Vazquez, P. Singh, A.V. Smirnov, D.D. Johnson, K. Youssef, and R. Arróyave, Acta Mater. 224, 117472 (2022).
- H. Sun, Z. Ding, D. Zhang, H. Zhou, S. Li, E.J. Lavernia, Y. Zhu, and W. Liu, Materialia 7, 100352 (2019).
- Z. Pei and J. Yin, *Mater. Des.* 172, 107759 (2019).
- R. Jaafreh, Y.S. Kang, K. Hamad, and J. Magnes, Alloys 11, 392 (2023)
- 38. Y. Chen, Y. Tian, Y. Zhou, D. Fang, X. Ding, J. Sun, and D. Xue, J. Alloys Compd. 844, 156159 (2020).
- S. Zhang, W. Yi, J. Zhong, J. Gao, Z. Lu, and L. Zhang, Materials 16, 306 (2023).
- M. Stricker, B. Yin, E. Mak, and W.A. Curtin, Phys. Rev. Mater. 4, 103602 (2020).
- C. Zou, J. Li, W.Y. Wang, Y. Zhang, D. Lin, R. Yuan, X. Wang, B. Tang, J. Wang, X. Gao, H. Kou, X. Hui, X. Zeng, M. Qian, H. Song, Z.-K. Liu, and D. Xu, Acta Mater. 202, 211 (2021).

- C. Tantardini and A.R. Oganov, Nat. Commun. 12, 2087
- C. Kittel, P. McEuen, and W.J. Sons, Introduction to Solid State Physics (John Wiley & Sons, Hoboken, NJ, 2015).
- F. Pedregosa, G. Varoquaux, A. Gramfort, V. Michel, B. Thirion, Ö. Grisel, M. Blondel, P. Prettenhofer, R. Weiss, V. Dubourg, J. Vanderplas, A. Passos, D. Cournapeau, M. Brucher, M. Perrot, and É. Duchesnay, J. Mach. Learn. Res. 12, 2825 (2011).
- T. Chen, C. Guestrin, Xgboost: A Scalable Tree Boosting System. Paper Presented at the 22nd ACM SIGKDD International Conference on Knowledge Discovery and Data Mining (2016), San Francisco, CA, USA (2016), pp. 785-794.
- 46. S.M. Lundberg and S.-I. Lee, Adv Neural Inf Process Syst, ed. by I. Guyon, U. Von Luxburg, S. Bengio, H. Wallach, R. Fergus, S. Vishwanathan, and R. Garnett (Curran Associates, Inc., 2017).
- A.E. Hoerl and R.W. Kennard, Technometrics 12, 55 (1970).
- G. Kresse and J. Furthmüller, Comput. Mater. Sci. 6, 15
- G. Kresse and J. Furthmüller, Phys. Rev. B 54, 11169 49.
- G. Kresse and J. Hafner, Phys. Rev. B 47, 558 (1993).
- G. Kresse and D. Joubert, *Phys. Rev. B* 59, 1758 (1999).
- V.L. Deringer, A.L. Tchougréeff, R. Dronskowski, and J. Phys, Chem. A. 115, 5461 (2011).
- S. Maintz, V. Deringer, A. Tchougréeff, and R. Dronskowski, 53. J. Comput. Chem. 37, 1030 (2016).

Publisher's Note Springer Nature remains neutral with regard to jurisdictional claims in published maps and institutional affiliations.

Springer Nature or its licensor (e.g. a society or other partner) holds exclusive rights to this article under a publishing agreement with the author(s) or other rightsholder(s); author selfarchiving of the accepted manuscript version of this article is solely governed by the terms of such publishing agreement and applicable law.